Physica B 614 (2021) 413029

Contents lists available at ScienceDirect

Physica B: Physics of Condensed Matter

journal homepage: http://www.elsevier.com/locate/physb

Electrical, photodiode, and DFT studies of newly synthesized π-conjugated BODIPY dye-based Au/BOD-Dim/n-Si device

Muhammet Ferit Şahin [a], Enis Taşcı [b], Mustafa Emrullahoğlu [c], Halil Gökce [b], Nihat Tuğluoğlu [a], Serkan Eymur [a,*]

[a] Department of Energy Systems Engineering, Giresun University, Giresun, Turkey
[b] Vocational School of Health Services, Giresun University, Giresun, Turkey
[c] Department of Photonics, İzmir Institute of Technology, İzmir, Turkey

ARTICLE INFO

Keywords:
Organic semiconductor
BODIPY
DFT
Schottky diode
Photodiode
Heterojunction

ABSTRACT

A π-conjugated 4,4-difluoro-4- bora-3a,4a-diaza-s-indacene (BODIPY) dimer (BOD-Dim) compound has been synthesized and characterized. The optimized molecular structure, the highest occupied molecular orbital (HOMO) and the lowest unoccupied molecular orbital (LUMO) simulations, and static isotropic polarizability of the isolated compound were computed via the Gaussian program. The simulated static dielectric constant value was calculated. The effect of the BOD-Dim interlayer on the diode characteristics of the Au/n-Si diode was investigated. The electrical and photovoltaic parameters of the Au/BOD-Dim/n-Si/In diode such as ideality factor (n), barrier height (Φ_B), open-circuit voltage (V_{oc}), short-circuit current (J_{sc}), photosensitivity (S), and photoresponsivity (R) have been investigated by current-voltage measurements at dark and under various illumination intensities. The possible current conduction mechanism has been examined through the forward bias ln(I_F)-ln(V_F) and ln(I_R)-$V_R^{1/2}$ characteristics. All obtained results confirmed that Au/BOD-Dim/n-Si/In diode exhibits a photovoltaic behavior and presents great potential as a photosensor for optoelectronic device applications.

1. Introduction

The interest on studies related to the development of solution processable small π-conjugated semiconducting organic molecules has been increased recently in view of their technological applications [1–3]. Due to their π-conjugated molecular structure which allows charge carriers to be transmitted via a hopping process, organic semiconductor have exciting electrical and optoelectronic properties. Also, in their low cost and easy preparation techniques and their chemical stability and tunable optical properties, organic semiconductors have been employed in electronic, optoelectronic, and photonic devices [2,4–13]. Organic semiconductors are thought to be alternatives to inorganic semiconductors, as they offer various properties such as mechanical flexibility, solubility in various organic solvents, easy processing for device manufacturing, chemical and thermal stability, and relatively low cost. Considering the abovementioned properties, it is not unexpected that the usage areas of organic semiconductors will expand further in the near future.

The interest on studies related to Schottky contacts obtained by contacting metals with semiconductors has been arisen in last decades due to their possible usage in several applications. It is known that the interface state densities at the metal semiconductor (MS) interface have a significant influence on the electrical parameters of a Schottky contact. Besides, the performance and stability of devices are sensitive to interfacial properties of metal-semiconductor contacts. There are many studies in the literature that reveal the advantages of using hybrid organic-inorganic heterojunction in a single structure for diode parameters. For instance, in the past few decades, metal-organic interlayer-semiconductor type Schottky barrier diodes which obtained by forming an organic semiconductor layer on an inorganic semiconductor have been made to improve the electrical characteristics of the device [10,11,14–24].

Organic semiconductors can be found either as small molecules, oligomers, or polymers. Organic dyes, in particular, are of widespread interest in the use of organic semiconductors due to their good solubility in different solvents which make them suitable for easy device

* Corresponding author.
E-mail address: serkan.eymur@giresun.edu.tr (S. Eymur).

https://doi.org/10.1016/j.physb.2021.413029
Received 25 February 2021; Received in revised form 26 March 2021; Accepted 27 March 2021
Available online 1 April 2021

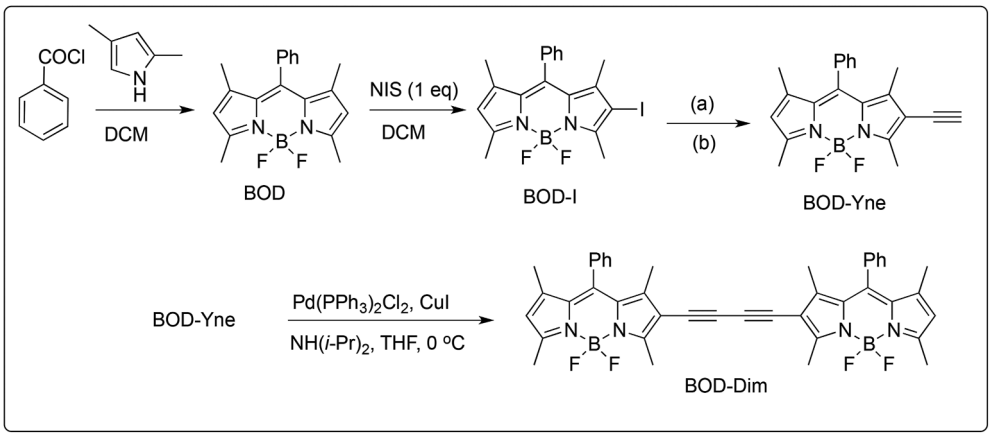

Fig. 1. Synthetic route of BOD-Dim compound.

fabrication via spin coating [14,16,18–20,22,25–27]. Among many semiconducting organic dyes in the last decades, derivatives of BODIPY, one of the most popular fluorescent dye, have emerged as an important class of materials that have high hole mobility due to their large π-conjugated structure [28–30]. Yet other advantages of BODIPY dyes are their high extinction coefficients, easy functionalization technique as well as good chemical and photochemical stabilities. In this respect, BODIPY dyes seem to be good candidates for organic semiconductors which can be useful for optoelectronic and photovoltaic devices. For these reasons, the BODIPY core which is a remarkable semiconducting structure has often been used for various applications such as dye-sensitized solar cells, photovoltaics, and organic electronics [29–32]. Among these studies, few studies on the effect of using π-conjugated BODIPY compounds as an interlayer on the structural and optical properties of Au/n-Si thin film were found in the literature [29, 33–35]. In this context, the synthesis of π-extended BODIPY derivatives with high semiconductivity level is still desired to show their potential in Schottky barrier diodes (SBDs).

The main aim of this study is to investigate the effect of π-extended BODIPY interlayer on the diode characteristics of the Au/n-Si diode. For this purpose, a π-extended BODIPY derivative (BOD-Dim) was designed and synthesized. Its chemical structure was confirmed by ^{1}H and ^{13}C spectroscopy. Then, Au/n-Si/BOD-Dim/In diode was fabricated by spin-coating technique, and its illumination dependence of electrical and photoelectrical properties were determined by using *I–V* measurements.

2. Experimental

2.1. Synthesis of BOD-Dim

BOD, BOD-I, and BOD-Yne compounds were synthesized according to literature (Fig. 1) [36]. Under argon atmosphere, BOD-Yne (90 mg, 0.26 mmol), $PdCl_2(PPh_3)_2$ (9.0 mg, 0.05 equiv.), and CuI (5.0 mg, 0.1 equiv.) were taken up in THF (4 mL) at 0 °C. Diisopropylamine (109 μL, 3.0 equiv.) was added, and the resulting mixture was stirred at ambient temperature for 45 min. Then, the mixture was heated to 40 °C for about 4 h. The mixture was diluted with Et_2O (25 mL) and washed with 1 M HCl (10 mL) and brine (10 mL). The organic layer was dried over $MgSO_4$, filtered and concentrated. The residue was purified by column chromatography on silica gel using EtOAc:hexane (1:7) as the eluent, which yield the pure BOD-Dim compound as purple solid (63.1 mg, 35% yield). ^{1}H NMR (400 MHz, $CDCl_3$): δ 7.51–7.49 (m, 6H), 7.26–7.24 (m, 4H), 6.05 (s, 2H), 2.65 (s, 6H), 2.57 (s, 6H), 1.44 (s, 6H), 1.39 (s, 6H). ^{13}C NMR (100 MHz, $CDCl_3$): δ 158.6, 157.6, 145.4, 144.0, 142.2, 134.5, 132.9, 129.9, 127.8, 122.5, 113.7, 80.2, 75.5, 14.8, 14.6, 13.6, 13.2.

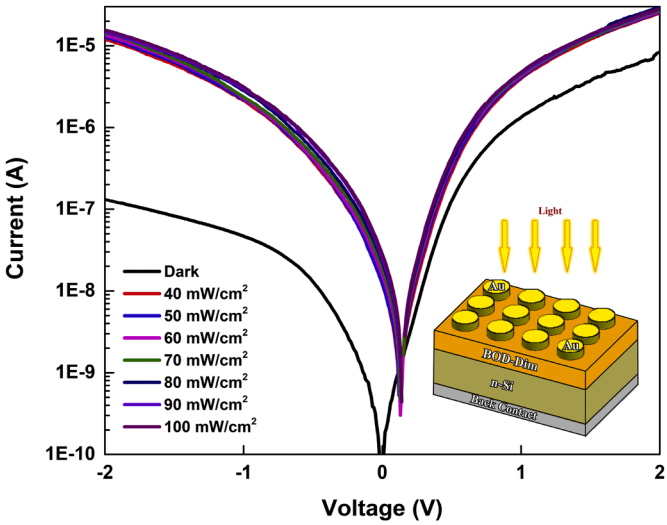

Fig. 2. *I–V* characteristics of the prepared diode. Inset shows the schematic representation of the fabricated diode.

2.2. Fabrication of Au/BOD-Dim/n-Si/In diode

The diode was prepared using n-type Si wafer and BOD-Dim organic material. To this aim, firstly, a n-type Si wafer was chemically cleaned using standard RCA cleaning procedures to eliminate the impurities and inherent oxide layer on surface. After cleaning procedure, 100 nm thickness indium (In) metal was evaporated on the Si wafer to prepare ohmic contact and then, it was thermally treated at 350 °C for 2 min in nitrogen atmosphere. After ohmic contact procedure, the solution of BOD-Dim organic thin film was coated on n-Si wafer by spin coating technique. Finally, Au metal dot contacts were prepared on the BOD-Dim film at a pressure of 10^{-6} torr by using a shadow mask. From the capacity of the accumulation region at 1 MHz, the thickness of BOD-Dim interfacial layer was found to be 229.6 nm. The *I–V* measurements of the diode were performed using a Keithley 2410 Source Meter in dark and under illumination intensity range of 40–100 mW/cm^2 using a solar simulator. Solar power meter was used to measure the intensity of the light.

3. Results and discussion

The *I–V* measurements were performed to investigate the current mechanism and obtain the main diode parameters. Fig. 2 shows the *I–V* characteristics of the diode in the dark and under various illumination

Table 1
The calculated ideality factor (n), reverse saturation current (I_o), barrier height (Φ_B) and series resistance (R_s) in dark and under different illumination levels.

Illumination intensity (mW/cm^2)	Region I			Region II		
	I_{o1} (A)	n_1	Φ_{B1} (eV)	I_{o2} (A)	n_2	Φ_{B2} (eV)
0	1.91×10^{-10}	2.66	0.907	4.41×10^{-9}	5.86	0.826
40	1.06×10^{-10}	1.92	0.922	7.37×10^{-9}	5.36	0.812
50	7.86×10^{-11}	1.72	0.930	9.44×10^{-9}	5.55	0.806
60	3.91×10^{-11}	1.44	0.948	1.11×10^{-8}	5.65	0.802
70	4.08×10^{-11}	1.43	0.947	1.28×10^{-8}	5.76	0.798
80	2.89×10^{-11}	1.32	0.956	1.24×10^{-8}	5.69	0.799
90	2.92×10^{-11}	1.31	0.957	1.64×10^{-8}	6.00	0.792
100	1.82×10^{-11}	1.21	0.968	1.55×10^{-8}	5.88	0.793

levels. As seen, the fabricated Au/Bod-Dim/n-Si/In diode has a good rectifying behavior under dark with a small leakage current in the reverse bias region which means that the diode shows a Schottky contact behavior. Under illumination conditions, the photocurrent in the reverse bias region is slightly higher than in the dark current. The value of current increases with increasing illumination level reveals that the Au/BOD-Dim/n-Si/In diode shows a photoconducting behavior. Under illumination of the sample, the *I–V* curve moves towards fourth quadrant representing that the produced photodiode is act as a generator of electricity due to the photogeneration of charges carriers [37–39]. According to Fig. 2, the forward bias semi-logarithmic *I–V* characteristics in dark and under different illumination intensities shows two different linear parts with different slopes in low voltages ($0.08<V<0.15$ V in dark and $0.17<V<0.25$ in light) and in mid-level voltages ($0.4<V<0.8$) which are called as regions I and II, respectively. The relation between *I* and *V* for non-ideal Schottky diodes ($V > 3kT/q$) with a series resistance for two linear regions in dark and under different illumination intensities is expressed according to the thermionic emission (TE) theory as follows [3,40,41]:

$$I = I_{01}\left[exp\left(\frac{q(V-IR_S)}{n_1 kT}\right)-1\right] + I_{02}\left[exp\left(\frac{q(V-IR_s)}{n_2 kT}\right)-1\right] \quad (1)$$

where n_1, n_2, T, q, V, and k are defined as ideality factor for regions I and II, temperature in Kelvin, electron charge, applied voltage and Boltzmann constant, respectively. I_{01} and I_{02} defined as the reverse saturation currents for regions I and II are given as,

$$I_{01} = AA^{*}T^{2}exp\left[-\frac{q\Phi_{B1}}{kT}\right] \quad (2a)$$

$$I_{02} = AA^{*}T^{2}exp\left[-\frac{q\Phi_{B2}}{kT}\right] \quad (2b)$$

where A and A* are defined as effective diode area and Richardson coefficient (112 A/cm^{2}K^2 for n-type Si), respectively. Φ_B is the effective barrier height which is determined by the following equation:

$$\Phi_B = \frac{kT}{q} ln\left(\frac{AA^{*}T^{2}}{I_0}\right) \quad (3)$$

According to Eq. (1), the straight-line intercept of the ln *I–V* plot at $V = 0$ gives I_0 value. The ideality factor which explains the departure of the current transport mechanism from the ideal TE model can be obtained from the slope of ln *I–V* characteristics according to the following equation:

$$n = \frac{q}{kT}\frac{dV}{d(lnI)} \quad (4)$$

The n, Φ_B, and I_0 values for dark and under different illumination conditions calculated using *I–V* plots and Eqs (1)–(4) for regions I and II were given in Table 1. The n and Φ_B values were found to be 2.66–5.86 and 0.907–0.826 eV in dark, respectively. Also, the n and Φ_B values were found to be 1.21–5.88 and 0.968–0.793 eV under 100 mW/cm^2 illumination level, respectively.

As seen, for region I, the n values have decreased with increasing illumination level due to increasing photo generated charge carriers under illumination in the interface of device [1,2,42]. The n value of

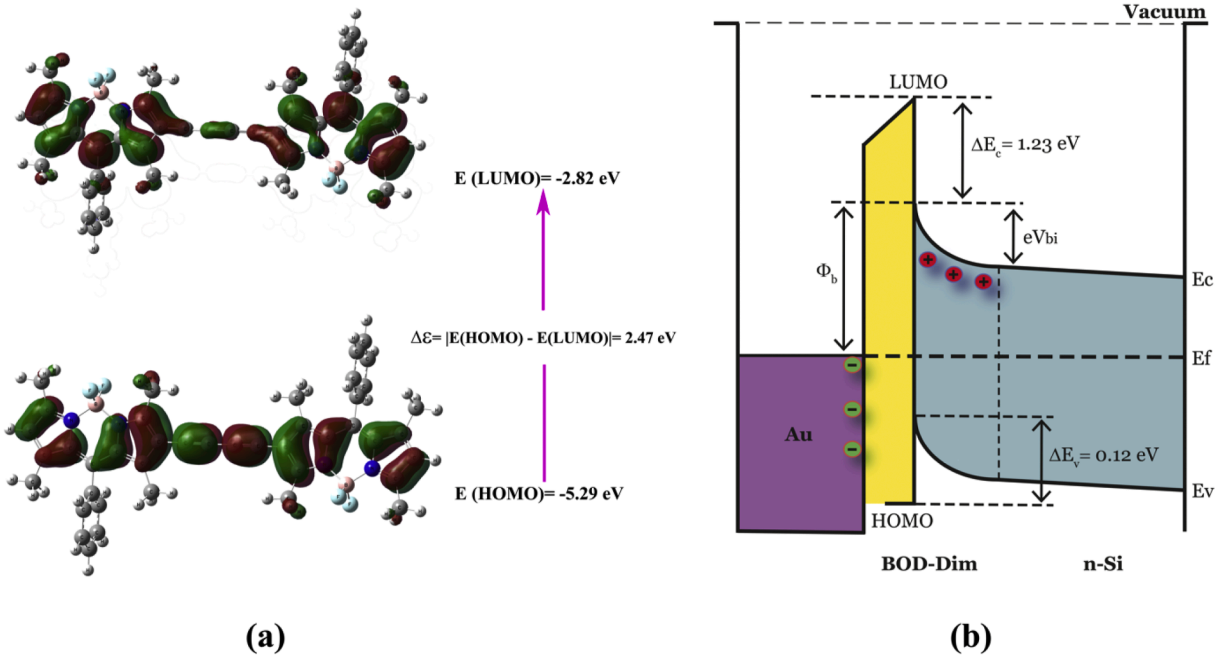

Fig. 3. (a) DFT computed energy the energy difference between the HOMO and LUMO of Bod-Dim. (b) Energy band diagram of Au/BOD-Dim/n-Si/In heterojunction device.

ideal diode should be equal to 1 for thermionic emission. However, the deviation of the experimental ideality factor from ideal *I–V* characteristics is attributed to the interface states, barrier inhomogeneity, and series resistance. A similar behavior of the light dependent ideality factor parameter for SBDs was reported in the literature [1,2,42].

To obtain detail information about the electronic structure, conductivity and ground state optimize molecular geometry of the BOD-Dim compound, Gaussian 09 program software [43] was used, and the optimized molecular structure, HOMO and LUMO simulations, static isotropic polarizability, and molar volume at the gas phase state of the isolated compound were computed. Starting molecular geometry was created via help of GaussView5 graphical interface program [44]. Then, the molecular structure optimization was obtained with the DFT-B3LYP/6-311G(d,p) computational level [45–47]. Based on optimized molecular structure, the static isotropic polarizability ($\alpha_{iso.} = \frac{1}{3}(\alpha_{xx} + \alpha_{yy} + \alpha_{zz})$) and molar volume ($V_M$) were obtained with the mentioned computational level. The keyword *tight* was used in all computations. The Clausius-Mossotti equation which used to compute the dielectric constant of any molecular system or medium depending on its polarizability and molar volume is expressed as:

$$\frac{\varepsilon_r - 1}{\varepsilon_r + 2} = \frac{4\pi N_A \alpha'}{3V_M} \tag{5}$$

where ε_r, V_M, and N_A are the dielectric constant and molar volume of the compound or medium, and Avogadro's constant, respectively. α' is the molecular polarizability volume defined in terms of the conventional polarizability α as $\alpha' = \alpha/4\pi\varepsilon_0$.

For our compound at the isolated gas phase state, the static isotropic polarizability ($\alpha_{iso.}$) and molar volume (V_M) values were computed as 762.1582 a_o^3 (or 1.1294 × 10^{-22} cm^3) and 500.076 cm^3/mol, respectively. According to the Clausius-Mossotti equation, the dielectric constant (ε_r) of the compound was found to be 4.98. The graphical presentation of the frontier molecular orbital energies i.e., HOMO, LUMO, and energy gap (Δε) for BOD-Dim are presented in Fig. 3 (a). As seen, the interfrontier molecular orbital energy gap (Δε) which provides information about the conductivity was calculated to be 2.47. Since the range of Δε for semiconductors is between 0.5–3.5 eV, the value of Δε (2.73 eV) for BOD-Dim shows that it can have a semiconducting behavior [48]. In the Au/BOD-Dim/n-Si/In device, the π-conjugated BOD-Dim organic compound inserted between metal and semiconductor, which acts as a physical barrier between the metal and the semiconductor, prevents direct contact of the metal with the silicon substrate [49,50]. Fig. 3 (b) shows the energy band diagram of the heterojunction device where ΔE_c is the difference in the energy between the LUMO and conduction band minimum of n-Si, ΔE_v is the valence-band offset, and eV_{bi} is the barrier to electron injection from n-Si through the junction. Since the obtained Φ_b values of Au/BOD-Dim/n-Si/In device (0.907–0.968 eV) are higher than the traditional Au/n-Si Schottky diodes (0.62 eV), it can be concluded that BOD-Dim organic layer can have an important effect on the electrical properties of the fabricated diode due to the local electronic states at the interface [49,50].

In metal-semiconductor contacts, another important parameter to determine that effects the diode performance is the presence of series resistance (R_s). To determine the Rs values for dark and under various illumination intensity, the forward bias *I–V* characteristics due to the thermionic emission of a Schottky diode with the series resistance were analyzed by using d*V*(d(ln*I*)) and *H*(*I*) functions introduced by Cheung and Cheung which defined a relation between R_s, *I* and *V* as [51,52]:

$$\frac{dV}{d(lnI)} = \frac{nkT}{q} + IR_s \tag{6}$$

and

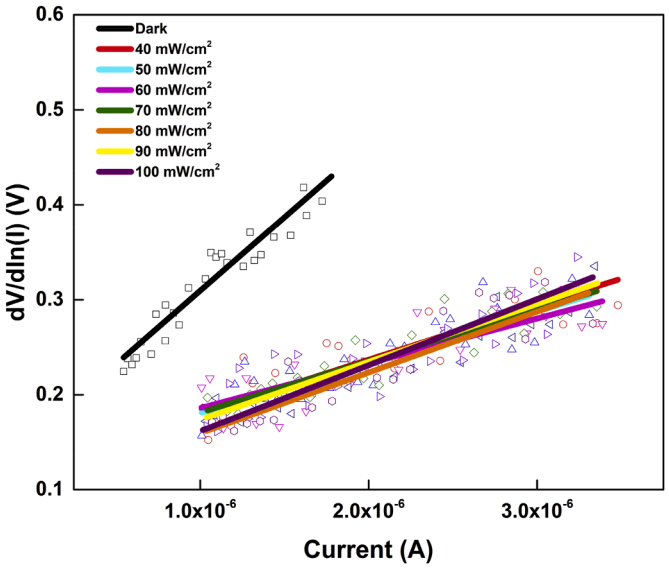

Fig. 4. d*V*/dln(*I*)–*I* plots of fabricated diode.

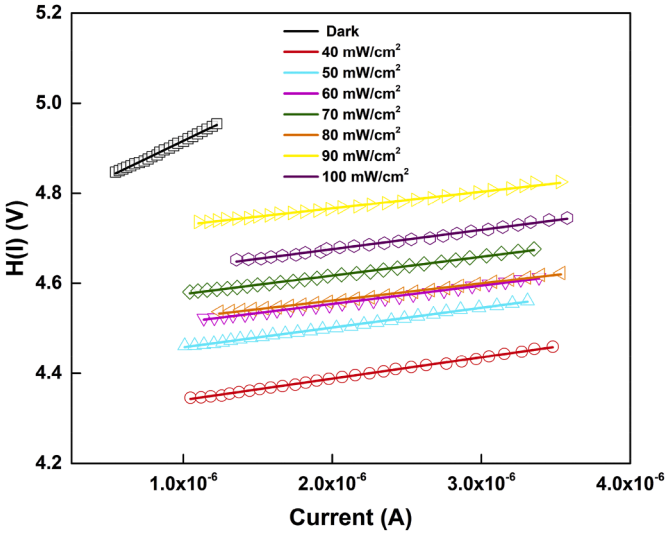

Fig. 5. *H*(*I*)–*I* plots of fabricated diode.

Table 2
Basic electrical parameters of the structure obtained from Cheung functions.

Illumination intensity (mW/cm²)	d*V*/d ln (I) − *I*		H(*I*)–*I*	
	R_s (kΩ)	*N*	R_s (kΩ)	Φ_B (eV)
0	154	6.19	158	0.812
40	56	4.93	47	0.801
50	53	5.09	44	0.795
60	47	5.56	41	0.792
70	54	5.08	42	0.787
80	64	3.82	38	0.788
90	61	4.52	37	0.782
100	69	3.68	43	0.781

$$H(I) = V - n\frac{kT}{q}\ln\left(\frac{I}{AA^*T^2}\right) = n\Phi_B + IR_s \tag{7}$$

First, the $dV/d(lnI)$-*I* plots for Au/BOD-Dim/n-Si/In heterojunction were drawn in Fig. 4. As can be seen, the plot of $dV/d(lnI)$ versus *I* is linear and its intercept and slope give *n*and R_s, respectively. The R_s

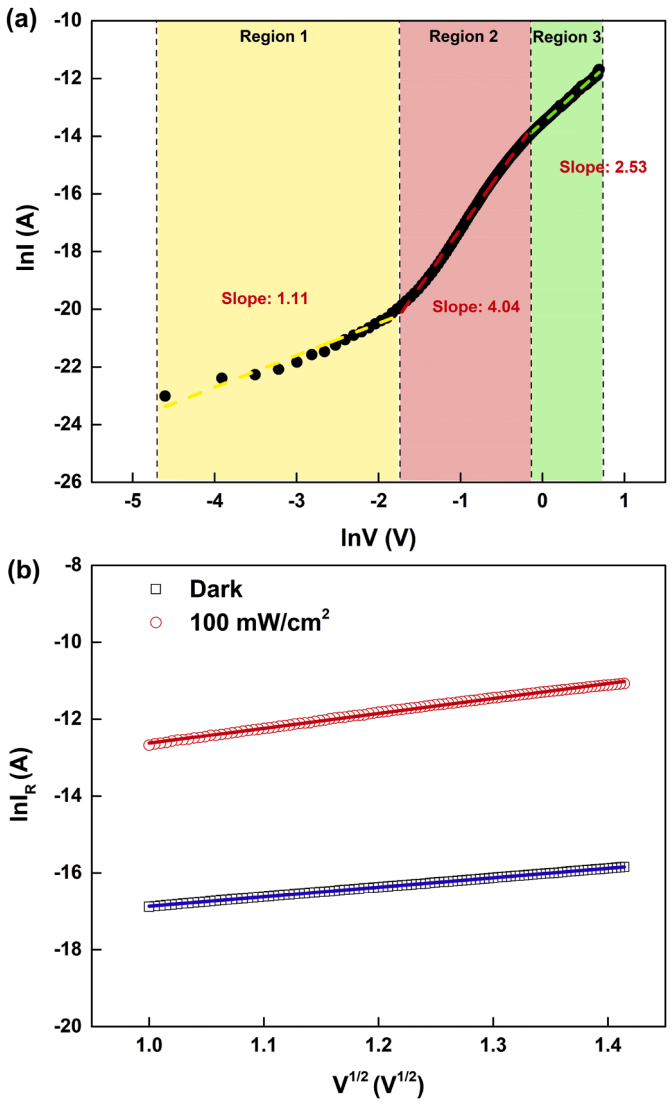

Fig. 6. (a) ln$I$-ln$V$ plot (b) ln (I_R)-$V^{1/2}$ plots of the Au/BOD-Dim/n-Si/In diode.

values were found to be 154 kΩ and 69 kΩ in dark and under 100 mW/cm^2 illumination level, respectively. Second, the $H(I)$-I plots for Au/BOD-Dim/n-Si/In heterojunction were drawn in Fig. 5. As can be seen, plot of $H(I)$ versus I is linear and its intercept and slope give Φ_B and R_s, respectively. The R_s values were found to be 158 kΩ and 43 kΩ in dark and under 100 mW/cm^2 illumination level, respectively. The junction parameters calculated from $dV/d(lnI)$ and $H(I)$ plots have been shown in Table 2 in dark and under different illumination intensity. The decrease in the value of R_s with the increase of light intensity can be attributed to the increase in free carrier concentration by incident light absorption.

In order to obtain detailed information about the conduction mechanisms which controls the junction behavior, the forward bias ln (I_F)-lnV_F and ln(I_R)-$V^{1/2}$ characteristics of the Au/BOD-Dim/n-Si/In diode were drawn in Fig. 6 (a) and (b), respectively. It has been known that the presence of deep traps at the interface changes the mobility and free carrier concentration, and these changes affect the slope of the I–V characteristics. Fig. 6 indicates three different regions that obeys $I \propto V^m$ relation where m values obtained from the slope of the ln$I$ - ln$V$ plot. In the region I ($-4.61 < \ln V < -1.77$), the current has a linear relation with the voltage with a slope of ~ 1.11, indicating the ohm's conduction mechanism. The slope of the region II ($-1.71 < \ln V < -0.15$) was found to be 4.04 which means I–V curve follows a power law, and the charge transport is governed by the trap-charge-limited

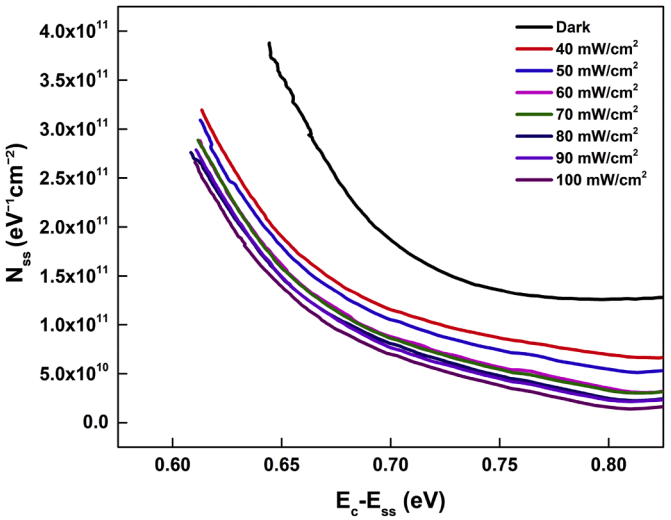

Fig. 7. N_{ss} distribution profiles as a function of E_c-E_{ss}.

current (TCLC). For region 3, ($-0.14 < \ln V < -0.69$), the value of m is about 2.53, and the current follows the relationship $I \propto V^2$ shows that the diode exhibits the space charge limited current (SCLC) mechanism [3,53–55].

For the reverse bias region, the current conduction mechanism of the Au/BOD-Dim/n-Si/In was examined by using two field lowering mechanism namely Schottky emission (SE) and Poole-Frenkel (PF) emission theories [56–58]. While the SE theory defines the relationship between I and V as Eq. (8a), the PF theory defines the same relations as Eq. (8b):

$$I_R = AA^* T^2 \exp\left(\frac{\beta_{SC} V^{1/2}}{kT\, d^{1/2}}\right) \tag{8a}$$

$$I_R = I_0 \exp\left(\frac{\beta_{PF} V^{1/2}}{kT\, d^{1/2}}\right) \tag{8b}$$

where β_{SC} and β_{PF} are the Schottky and Poole-Frenkel field lowering coefficients, respectively. As seen in Eqs. (8a) and (8b), the theoretical values of these coefficients can be expressed as follow:

$$2\beta_{SC} = \beta_{PF} = \left(\frac{q^3}{\varepsilon_r \varepsilon_0 \pi}\right)^{1/2} \tag{9}$$

where ε_r is the permittivity of the interfacial layer. The theoretical values of β_{PF} and β_{SC} are found as 6.80×10^{-5} and 3.40×10^{-5} eV m$^{1/2}$ V$^{-1/2}$, respectively. As seen in Fig. 6. (b), the ln(I_R) versus $V^{1/2}$ plots of the prepared diode showed a linear region for dark and under 100 mW/cm^2 illumination level. The experimentally calculated β values obtained from the slope of Fig. 5, (b) were found to be 3.94×10^{-4} and 6.19×10^{-4} eV m$^{1/2}$ V$^{-1/2}$ for dark and under 100 mW/cm^2 illumination level, respectively. According to these obtained results, it can be said that the dominant conduction mechanism for the Au/BOD-Dim/n-Si/In diode is the SE mechanism as the value of β is closer to the SE coefficient [56–58].

In addition to R_s, the deviation of I–V characteristics of SBDs from the linearity at high forward biases is also attributed to the density of the interface states which is located between the interfacial layer and the semiconductor interface. Card and Rhoderick simply defined the relation between N_{ss} and ideality factor for n-type Schottky diode as [54,59]:

$$N_{ss}(V) = \frac{1}{q}\left[\frac{\varepsilon_i}{\delta_i}(n(V) - 1) - \frac{\varepsilon_s}{W_D}\right] \tag{10}$$

where δ_i is the thickness of interface layer, W_D is space charge width, ε_s

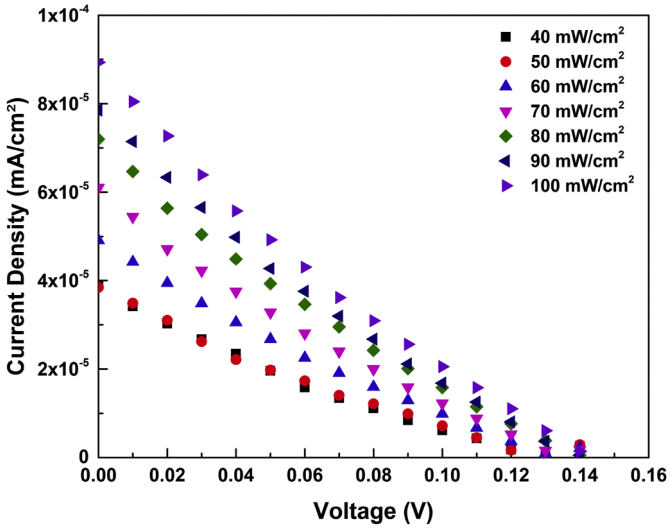

Fig. 8. Plot of *J-V* curves for different illumination intensities.

and ε_i are dielectric constant of semiconductor and interface, respectively. In n-type semiconductor, the energy density distribution (E_C-E_{SS}) is defined as:

$$E_c - E_{ss} = q(\Phi_e - V), \Phi_e = \Phi_B + \beta V = \Phi_B + \left(1 - \frac{1}{n(V)}\right)V \tag{11}$$

where Φ_e is the effective barrier height, q is the electron charge and V is the applied voltage drop across the depletion layer. Fig. 7 shows the N_{ss} energy distribution curves of the Au/Bod-Dim/n-Si/In diode for dark and under different illumination intensities. As can be seen in Fig. 7, the values of interface state density N_{ss} vary from E_c - 0.6 eV to E_c - 0.83 eV for dark and under different illumination intensities, respectively. The N_{ss} values for dark decreases exponentially with bias from 4.39×10^{11} eV^{-1} cm^{-2} at (E_c - 0.636) eV to 1.27×10^{11} eV^{-1} cm^{-2} at (E_c - 0.827) eV. This energy range is higher than the mid-gap of Si. In other words, these states seem to deep-electronic level rather than shallow (donor-type) states [60]. The values of N_{ss} decreased with the increasing illumination level. These observations indicated that the interface state densities are strongly dependent on illumination level and applied voltage. These observations also showed the rearrangement of the molecular metal-semiconductor interface under the effect of illumination.

Since the Au/BOD-Dim/n-Si/In diode is light sensitive, as said earlier and shown in Fig. 2, the photosensitive behavior of the diode was also analyzed under various illumination intensities. Fig. 8 shows the forward current density - applied voltage (*J-V*) characteristics of the Au/BOD-Dim/n-Si/In diode under various illumination intensity. The main photovoltaic parameters of the diode were obtained for various illumination intensities and presented in Table 3. As seen, the value of open-circuit voltage (V_{oc}) changed slightly with illumination while the value of short circuit current density (J_{sc}) increased with increasing light illumination intensity which can be attributed to the increasing in free carrier concentration due to incident light absorption. The value of fill factor (*FF*) was also found to decrease as illumination intensity increased.

Photosensitivity (*S*) and photoresponsivity (*R*), one of the important parameters used to investigate the photosensitive behavior of the diodes in more detail, were determined by the following relations [61–63]:

$$S = \frac{I_{ph}}{I_{dark}} \tag{12}$$

and

$$R = \frac{I_{ph}}{P.A} \tag{13}$$

where I_{ph}, I_{dark}, P, and A is the generated photocurrent, the dark current, power of the incident light and active area, respectively. For the Au/BOD-Dim/n-Si/In diode, the all *S* and *R* values obtained from Eqs (12) and (13) under different illumination intensities, at −2 V were listed in Table 2. As can be seen, there is an increase in the *S* values with increasing illumination intensities which indicate that the prepared diode is sensitive to illumination intensities and might exhibit photoconductivity effect. The relation between ln I_{ph} and ln P was also examined to get more information about the photoconduction mechanism of the Au/BOD-Dim/n-Si/In diode. The variation of the photocurrent against light intensity is given by the following relation:

$$I_{ph} = \gamma P^{\beta} \tag{14}$$

where γ value is a constant, β is an exponent which is determined from the slope of the ln I_{ph} vs. ln P plot. The plot of ln I_{ph} vs. ln P of Au/BOD-Dim/n-Si/In diode is given in Fig. 9. The β value which describes whether the process of recombination is monomolecular or bimolecular, for the Au/BOD-Dim/n-Si/In diode was found as 0.27. This shows that

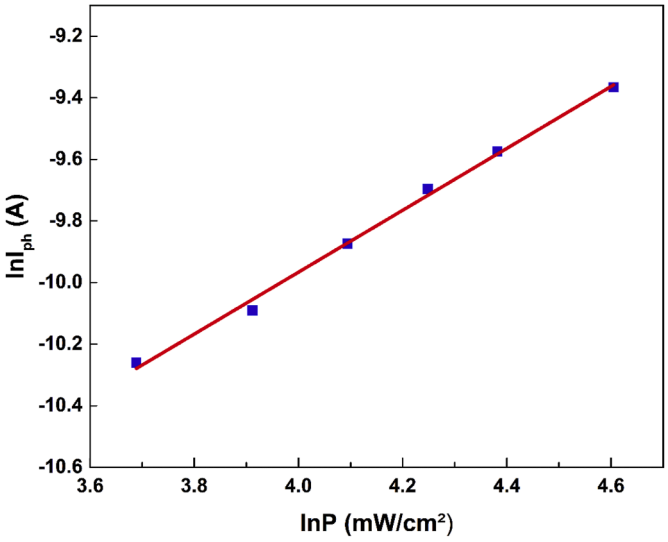

Fig. 9. lnI_{ph} - ln$P$ plot of the Au/BOD-Dim/n-Si/In diode.

Table 3
The photodiode parameters of the Au/BOD-Dim/n-Si/In device under various illumination levels.

Power (mW/cm^2)	V_{oc} (V)	J_{sc}(μA/cm^2)	V_{max} (V)	I_{max} (μA)	*FF*	P_{max} (mW/cm^2) x10^{-5}	*S* (at V_R = 2 V)	*R* (at V_R = 2 V)
40	0.12	0.39	0.05	0.16	20.97	0.98	90.18	0.020
50	0.13	0.39	0.06	0.17	20.79	1.04	97.03	0.016
60	0.13	0.49	0.06	0.22	21.16	1.35	101.8	0.014
70	0.13	0.61	0.06	0.28	21.22	1.68	106.9	0.012
80	0.14	0.72	0.06	0.34	20.61	2.08	114.7	0.011
90	0.14	0.78	0.07	0.32	20.34	2.24	110.0	0.010
100	0.15	0.89	0.07	0.36	20.23	2.53	116.7	0.010

the photoconduction mechanism might be controlled by the bimolecular recombination mechanism [64–66].

4. Conclusion

In this study, the electrical and photoelectrical properties of organic BODIPY dye-based Au/BOD-Dim/n-Si/In hybrid diode have been studied in dark and under various illumination intensities by using the forward and reverse bias *I–V* measurements. Experimental results showed that the fabricated diode showed good rectification properties, and the main diode parameters are strongly dependent upon illumination intensity and applied bias voltage. For instance, the ideality factor of the diode decreased with increasing illumination intensity. Moreover, the series resistance values obtained by dV/d(ln$I$) function of Cheung method have been found to be 154 kΩ and 69 kΩ in dark and under 100 mW/cm^2 illumination level, respectively. The values of N_{ss} decreased as the illumination level increased which indicates the possible rearrangement of the molecular metal-semiconductor interface under the effect of the illumination. The analysis of ln$I$-ln$V$ and ln(I_R)-$V^{1/2}$ plots showed that the dominant current conduction mechanism governed by the SCLC and TCLC at forward bias and the Schottky emission (SE) effect was found to be dominant in the reverse direction. The main photosensitive behavior of the diode such as V_{oc}, J_{sc}, V_{max}, J_{max}, and *FF* have also been analyzed under various illumination intensities by the *J-V* characteristics. The all obtained results indicate that the Au/BOD-Dim/n-Si/In diode shows a photovoltaic behavior and presents great potential in optoelectronic device applications.

Credit author statement

M. F. Şahin: Investigation, Experiment, Formal analysis, Visualization, Writing – original draft, E. Taşcı; : Investigation, Experiment, Visualization, Writing – original draft, M. Emrullahoğlu: Investigation, Experiment, Formal analysis, Visualization, Writing – original draft, H. Gökce: Investigation, Formal analysis, Visualization, Writing – original draft, N. Tuğluoğlu: Supervision, Resources, Investigation, Writing – original draft, Formal analysis, Experimental measurement, Writing – review & editing. S. Eymur: Project administration, Supervision, Resources, Investigation, Writing – original draft, Visualization, Writing – review & editing,

Declaration of competing interest

The authors declare that they have no known competing financial interests or personal relationships that could have appeared to influence the work reported in this paper.

References

[1] W. Brütting, Physics of Organic Semiconductors, Wiley-VCH, Weinheim, 2005.
[2] W. Hu, F. Bai, X. Gong, X. Zhan, H. Fu, et al., Organic Optoelectronics, Wiley-VCH, Weinheim, 2013.
[3] S.M. Sze, K.K. Ng, Physics of Semiconductor Devices, Wiley-Interscience, Hoboken, N.J., 2007.
[4] A. Eroglu, S. Demirezen, Y. Azizian-Kalandaragh, S. Altindal, A comparative study on the electrical properties and conduction mechanisms of Au/n-Si Schottky diodes with/without an organic interlayer, J. Mater. Sci. Mater. Electron. 31 (2020) 14466, https://doi.org/10.1007/s10854-020-04006-1.
[5] A.G. Imer, O. Karaduman, F. Yakuphanoglu, Controlling of the photosensing properties of Al/DMY/p-Si heterojunctions by the interface layer thickness, Synth. Met. 221 (2016) 114, https://doi.org/10.1016/j.synthmet.2016.08.014.
[6] F.M. Jin, Z.S. Su, B. Chu, P.F. Cheng, J.B. Wang, et al., Interface engineering of organic Schottky barrier solar cells and its application in enhancing performances of planar heterojunction solar cells, Sci. Rep. 6 (2016), https://doi.org/10.1038/srep26262.
[7] O. Pakma, S. Cavdar, H. Koralay, N. Tugluoglu, O.F. Yuksel, Improvement of diode parameters in Al/n-Si Schottky diodes with Coronene interlayer using variation of the illumination intensity, Physica B 527 (2017) 1, https://doi.org/10.1016/j.physb.2017.09.101.
[8] I.S. Yahia, H.Y. Zahran, F.H. Alamri, M.A. Manthrammel, S. AlFaify, et al., Microelectronic properties of the organic Schottky diode with pyronin-Y: admittance spectroscopy, and negative capacitance, Physica B 543 (2018) 46, https://doi.org/10.1016/j.physb.2018.05.011.
[9] M. Yildirim, A. Erdogan, O.F. Yuksel, M. Kus, M. Can, et al., The synthesis of 4,4-(9,9-dioctyl-9H-fluorene-2,7-diyl)bis(N,N-diphenylaniline) organic semiconductor and use of it as an interlayer on Au/n-Si diode, J. Mater. Sci. Mater. Electron. 30 (2019) 10408, https://doi.org/10.1007/s10854-019-01382-1.
[10] O.F. Yuksel, N. Tugluoglu, H. Safak, Z. Nalcacigil, M. Kus, et al., Analysis of temperature dependent electrical properties of Au/perylene-diimide/n-Si Schottky diodes, Thin Solid Films 534 (2013) 614, https://doi.org/10.1016/j.tsf.2013.02.042.
[11] S. Karadeniz, B. Baris, O.F. Yuksel, N. Tugluoglu, Analysis of electrical properties of Al/p-Si Schottky contacts with and without rubrene layer, Synth. Met. 168 (2013) 16, https://doi.org/10.1016/j.synthmet.2013.01.012.
[12] S. Demirezen, H.G. Çetinkaya, M. Kara, F. Yakuphanoğlu, Ş. Altındal, Synthesis, electrical and photo-sensing characteristics of the Al/(PCBM/NiO: ZnO)/p-Si nanocomposite structures, Sens. Actuators, A 317 (2021) 112449, https://doi.org/10.1016/j.sna.2020.112449.
[13] A. Tataroğlu, Ş. Altındal, Y. Azizian-Kalandaragh, Electrical and photoresponse properties of CoSO4-PVP interlayer based MPS diodes, J. Mater. Sci. Mater. Electron. 31 (2020) 11665, https://doi.org/10.1007/s10854-020-03718-8.
[14] K. Hunger, Industrial Dyes: Chemistry, Properties, Applications, Wiley-VCH, Weinheim, 2002.
[15] A.A.M. Farag, I.S. Yahia, Rectification and barrier height inhomogeneous in Rhodamine B based organic Schottky diode, Synth. Met. 161 (2011) 32, https://doi.org/10.1016/j.synthmet.2010.10.030.
[16] I.V. Klimovich, L.I. Leshanskaya, S.I. Troyanov, D.V. Anokhin, D.V. Novikov, et al., Design of indigo derivatives as environment-friendly organic semiconductors for sustainable organic electronics, J. Mater. Chem. C 2 (2014) 7621, https://doi.org/10.1039/C4TC00550C.
[17] A. Tombak, Y.S. Ocak, S. Asubay, T. Kilicoglu, F. Ozkahraman, Fabrication and electrical properties of an organic-inorganic device based on Coumarin 30 dye, Mater. Sci. Semicond. Process. 24 (2014) 187, https://doi.org/10.1016/j.mssp.2014.03.004.
[18] T.D. Kim, K.S. Lee, D–A conjugated molecules for optoelectronic applications, Macromol. Rapid Commun. 36 (2015) 943, https://doi.org/10.1002/marc.201400749.
[19] C. Wang, Z. Zhang, Y. Wang, Quinacridone-based π-conjugated electronic materials, J. Mater. Chem. C 4 (2016) 9918, https://doi.org/10.1039/C6TC03621J.
[20] J.-F. Morin, Recent advances in the chemistry of vat dyes for organic electronics, J. Mater. Chem. C 5 (2017) 12298, https://doi.org/10.1039/C7TC03926C.
[21] A.G. Imer, E. Kaya, A. Dere, A.G. Al-Sehemi, A.A. Al-Ghamdi, et al., Illumination impact on the electrical characteristics of Au/Sunset Yellow/n-Si/Au hybrid Schottky diode, J. Mater. Sci. Mater. Electron. 31 (2020) 14665, https://doi.org/10.1007/s10854-020-04029-8.
[22] C. Wang, X. Zhang, W. Hu, Organic photodiodes and phototransistors toward infrared detection: materials, devices, and applications, Chem. Soc. Rev. 49 (2020) 653, https://doi.org/10.1039/C9CS00431A.
[23] G. Ersoz, I. Yucedag, S. Bayrakdar, S. Altindal, A. Gumus, Investigation of photo-induced effect on electrical properties of Au/PPy/n-Si (MPS) type Schottky barrier diodes, J. Mater. Sci. Mater. Electron. 28 (2017) 6413, https://doi.org/10.1007/s10854-016-6326-z.
[24] H.E. Lapa, A. Kökce, D.A. Aldemir, A.F. Özdemir, Ş. Altındal, Effect of illumination on electrical parameters of Au/(P3DMTFT)/n-GaAs Schottky barrier diodes, Indian J. Phys. 94 (2020), https://doi.org/10.1007/s12648-019-01644-y, 1901.
[25] R. Stalder, J. Mei, K.R. Graham, L.A. Estrada, J.R. Reynolds, Isoindigo, a versatile electron-deficient unit for high-performance organic electronics, Chem. Mater. 26 (2014) 664, https://doi.org/10.1021/cm402219v.
[26] S. Demirezen, S. Altındal Yerişkin, A detailed comparative study on electrical and photovoltaic characteristics of Al/p-Si photodiodes with coumarin-doped PVA interfacial layer: the effect of doping concentration, Polym. Bull. 77 (2020) 49, https://doi.org/10.1007/s00289-019-02704-3.
[27] A.A.M. Farag, A.M. Mansour, A.H. Ammar, M.A. Rafea, Characterization of electrical and optical absorption of organic based methyl orange for photovoltaic application, Synth. Met. 161 (2011) 2135, https://doi.org/10.1016/j.synthmet.2011.08.015.
[28] Y.Q. Fan, J.J. Zhang, Z.Y. Hong, H.Y. Qiu, Y. Li, et al., Architectures and applications of BODIPY-based conjugated polymers, Polymers 13 (2021) 30, https://doi.org/10.3390/polym13010075.
[29] D. Ho, R. Ozdemir, H. Kim, T. Earmme, H. Usta, et al., BODIPY-based semiconducting materials for organic bulk heterojunction photovoltaics and thin-film transistors, Chempluschem 84 (2019) 18, https://doi.org/10.1002/cplu.201800543.
[30] M. Poddar, R. Misra, Recent advances of BODIPY based derivatives for optoelectronic applications, Coord. Chem. Rev. 421 (2020) 22, https://doi.org/10.1016/j.ccr.2020.213462.
[31] J.J. Chen, S.M. Conron, P. Erwin, M. Dimitriou, K. McAlahney, et al., High-efficiency BODIPY-based organic photovoltaics, ACS Appl. Mater. Interfaces 7 (2015) 662, https://doi.org/10.1021/am506874k.
[32] A. Loudet, K. Burgess, BODIPY dyes and their derivatives: syntheses and spectroscopic properties, Chem. Rev. 107 (2007) 4891, https://doi.org/10.1021/cr078381n.
[33] M. Ozdemir, D. Choi, G. Kwon, Y. Zorlu, B. Cosut, et al., Solution-processable BODIPY-based small molecules for semiconducting microfibers in organic thin-film transistors, ACS Appl. Mater. Interfaces 8 (2016) 14077, https://doi.org/10.1021/acsami.6b02788.

[34] A. Tataroğlu, A.G. Al-Sehemi, M. Özdemir, R. Özdemir, H. Usta, et al., Frequency and electric field controllable photodevice: FYTRONIX device, Phys. B Condens. Matter 519 (2017) 53, https://doi.org/10.1016/j.physb.2017.05.046.
[35] T. Kilicoglu, Y.S. Ocak, Electrical and photovoltaic properties of an organic-inorganic heterojunction based on a BODIPY dye, Microelectron. Eng. 88 (2011) 150, https://doi.org/10.1016/j.mee.2010.10.001.
[36] M. Üçüncü, E. Karakuş, E. Kurulgan Demirci, M. Sayar, S. Dartar, et al., BODIPY–Au(I): a photosensitizer for singlet oxygen generation and photodynamic therapy, Org. Lett. 19 (2017) 2522, https://doi.org/10.1021/acs.orglett.7b00791.
[37] I.M. El Radaf, A.M. Mansour, G.B. Sakr, Fabrication, electrical and photovoltaic characteristics of CuInGeSe4/n-Si diode, J. Semiconduct. 39 (2018), https://doi.org/10.1088/1674-4926/39/12/124010.
[38] A.A.M. Farag, W.G. Osiris, A.H. Ammar, A.M. Mansour, Electrical and photosensing performance of heterojunction device based on organic thin film structure, Synth. Met. 175 (2013) 81, https://doi.org/10.1016/j.synthmet.2013.04.030.
[39] A.A.M. Farag, H.S. Soliman, A.A. Atta, Analysis of dark and photovoltaic characteristics of Au/Pyronine G(Y)/p-Si/Al heterojunction, Synth. Met. 161 (2012) 2759, https://doi.org/10.1016/j.synthmet.2011.10.017.
[40] U. Akin, S. Sayin, N. Tugluoglu,O. F. Yuksel, Investigation of Optical and Diode Parameters of 9- (5-Nitropyridin-2-Aminoethyl) Iminiomethyl -Anthracene Thin Film, J. Electron. Mater., https://doi.org/10.1007/s11664-020-08690-x.
[41] A.A.M. Farag, F.S. Terra, G.M. Mahmoud, A.M. Mansour, Study of Gaussian distribution of inhomogeneous barrier height for n-InSb/p-GaAs heterojunction prepared by flash evaporation, J. Alloys Compd. 481 (2009) 427, https://doi.org/10.1016/j.jallcom.2009.03.004.
[42] S.S. Li, Semiconductor Physical Electronics, second ed., Springer-Verlag New York, New York, 2006.
[43] M.J. Frisch, G.W. Trucks, H.B. Schlegel, G.E. Scuseria, M.A. Robb, et al., Gaussian 09, Revision C.01, Gaussian Inc, Wallingford, CT, 2009.
[44] R. Dennington, T. Keith, J. Millam, GaussView, Version 5, Shawnee Mission KS, Semichem Inc, 2009.
[45] Y. Sert, G.A. El-Hiti, H. Gökce, F. Ucun, B.F. Abdel-Wahab, et al., DFT, molecular docking and experimental FT-IR, laser-Raman, NMR and UV investigations on a potential anticancer agent containing triazole ring system, J. Mol. Struct. 1211 (2020) 128077, https://doi.org/10.1016/j.molstruc.2020.128077.
[46] A.J. Thakkar, S.P. McCarthy, Toward improved density functionals for the correlation energy, J. Chem. Phys. 131 (2009), https://doi.org/10.1063/1.3243845.
[47] A.D. Becke, DENSITY-FUNCTIONAL thermochemistry .3. The role OF exact exchange, J. Chem. Phys. 98 (1993) 5648, https://doi.org/10.1063/1.464913.
[48] P.W. Atkins, M.E. Hagerman, D.F. Shriver, Inorganic Chemistry, Oxford Univ. Press, Oxford, 2010.
[49] L.S. Hung, C.H. Chen, Recent progress of molecular organic electroluminescent materials and devices, Mater. Sci. Eng. R Rep. 39 (2002) 143, https://doi.org/10.1016/S0927-796X(02)00093-1.
[50] D.R.T. Zahn, T.U. Kampen, H. Méndez, Transport gap of organic semiconductors in organic modified Schottky contacts, Appl. Surf. Sci. (2003) 212–213, https://doi.org/10.1016/S0169-4332(03)00125-9, 423.
[51] A.A.M. Farag, F.S. Terra, A. Ashery, A.M. Mansour, Structural and electrical characteristics of n-InSb/p-GaAs heterojunction prepared by liquid phase epitaxy, J. Alloys Compd. 615 (2014) 604, https://doi.org/10.1016/j.jallcom.2014.06.058.
[52] N. Tugluoglu, H. Koralay, K.B. Akgul, S. Cavdar, Detailed analysis of device parameters by means of different techniques in Schottky devices, J. Electron. Mater. 45 (2016) 3859, https://doi.org/10.1007/s11664-016-4580-8.
[53] H. Cetinkaya, S. Altindal, I. Orak, I. Uslu, Electrical characteristics of Au/n-Si (MS) Schottky Diodes (SDs) with and without different rates (graphene + Ca1.9Pr0.1Co4Ox-doped poly(vinyl alcohol)) interfacial layer, J. Mater. Sci. Mater. Electron. 28 (2017) 7905, https://doi.org/10.1007/s10854-017-6490-9.
[54] M. Benhaliliba, I. Missoum, S. Ozcelik, T. Asar, Optical filter and electrical behavior of innovative Au/ZnPc/Si/Al organic heterojunction, Optik (2020) 206, https://doi.org/10.1016/j.ijleo.2019.163629.
[55] E.M. El-Menyawy, A.M. Mansour, N.A. El-Ghamaz, S.A. El-Khodary, Electrical conduction mechanisms and thermal properties of 2-(2, 3-dihydro-1,5-dimethyl-3-oxo-2-phenyl-1H-pyrazol-4-ylimino)-2-(4-nitroph enyl)acetonitrile, Physica B 413 (2013) 31, https://doi.org/10.1016/j.physb.2012.12.030.
[56] M. Keskin, A. Akkaya, E. Ayyildiz, A.U. Oksuz, M.O. Karakus, Investigation of the temperature-dependent electrical properties of Au/PEDOT:WO3/p-Si hybrid device, J. Mater. Sci. Mater. Electron. 30 (2019) 16676, https://doi.org/10.1007/s10854-019-02048-8.
[57] K.A. Nasyrov, V.A. Gritsenko, Transport mechanisms of electrons and holes in dielectric films, Phys. Usp. 56 (2013) 999, https://doi.org/10.3367/UFNe.0183.201310h.1099.
[58] M.A. Rafiq, Carrier transport mechanisms in semiconductor nanostructures and devices, J. Semiconduct. 39 (2018) 61002, https://doi.org/10.1088/1674-4926/39/6/061002.
[59] T. Kilicoglu, M.E. Aydina, G. Topal, M.A. Ebeoglu, H. Saygili, The effect of a novel organic compound chiral macrocyclic tetraamide-I interfacial layer on the calculation of electrical characteristics of an Al/tetraamide-I/p-Si contact, Synth. Met. 157 (2007) 540, https://doi.org/10.1016/j.synthmet.2007.06.001.
[60] Z. Caldiran, A.R. Deniz, S. Aydogan, A. Yesildag, D. Ekinci, The barrier height enhancement of the Au/n-Si/Al Schottky barrier diode by electrochemically formed an organic Anthracene layer on n-Si, Superlattice. Microst. 56 (2013) 45, https://doi.org/10.1016/j.spmi.2012.12.004.
[61] U. Akin, O.F. Yuksel, E. Tasci, N. Tugluoglu, Fabrication of a new hybrid coronene/n-Si structure by using spin coating technique and its photoresponse and admittance spectroscopy studies, Siliconindia 12 (2020) 1399, https://doi.org/10.1007/s12633-019-00233-2.
[62] A.A. Hendi, Electrical and photoresponse properties of graphene oxide: ZnO/Si photodiodes, J. Alloys Compd. 647 (2015) 259, https://doi.org/10.1016/j.jallcom.2015.06.002.
[63] I.M. El Radaf, M. Nasr, A.M. Mansour, Structural, electrical and photovoltaic properties of CoS/Si heterojunction prepared by spray pyrolysis, Mater. Res. Express 5 (2018), https://doi.org/10.1088/2053-1591/aaa25e.
[64] R. Murdey, N. Sato, Photocurrent Action Spectra of Organic Semiconductors, 2015.
[65] F. Aslan, H. Esen, F. Yakuphanoglu, Electrical and fotoconducting characterization of Al/coumarin:ZnO/Al novel organic-inorganic hybrid photodiodes, J. Alloys Compd. 789 (2019) 595, https://doi.org/10.1016/j.jallcom.2019.03.090.
[66] A. Boutelala, F. Bourfa, M. Mahtali, Effect of light on electrical and photoelectrical characteristics of Al/TiO2/p-Si Schottky diode, J. Mater. Sci. Mater. Electron. 31 (2020) 11379, https://doi.org/10.1007/s10854-020-03687-y.